Electronic Supplementary Material (ESI) for Nanoscale.

Electronic Supplementary Information

Transformation of Carbon Dioxide into Carbon Nanotubes for Enhanced Ion Transport and Energy Storage

*Gi Mihn Kim, Won-Gwang Lim, Dohyung Kang, Jae Hyun Park, Hyunjoo Lee, Jinwoo Lee, and Jae W. Lee**

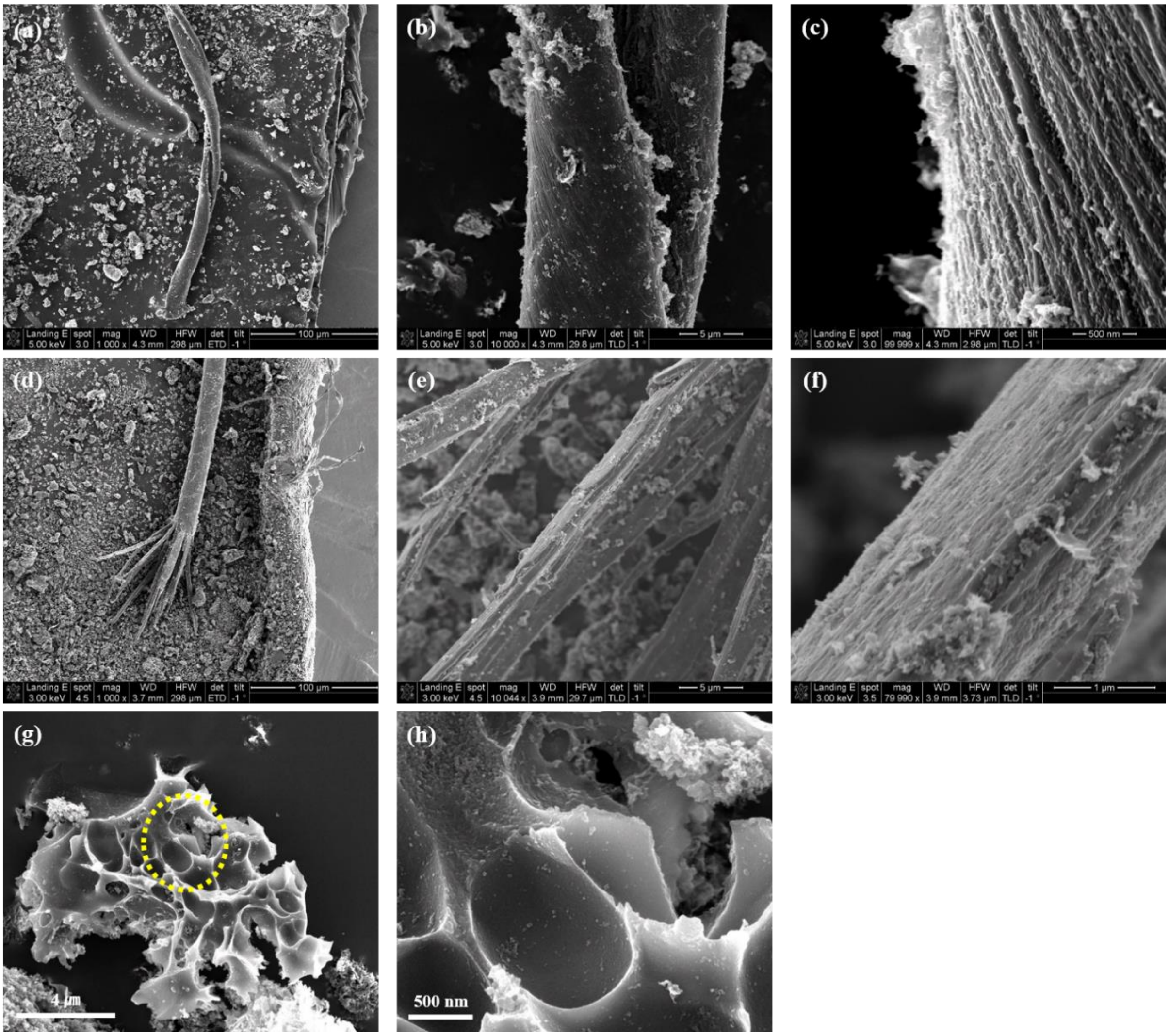

Figure S1. SEM images of (a-c) CC10 and (d-f) CC5 to show the CNT fiber structure. From (a) to (c) (or from (d) to (f)), the image becomes high in magnification. (g, h) SEM images of irregular porous carbon part in CC10. The yellow dashed circles represent the magnified area.

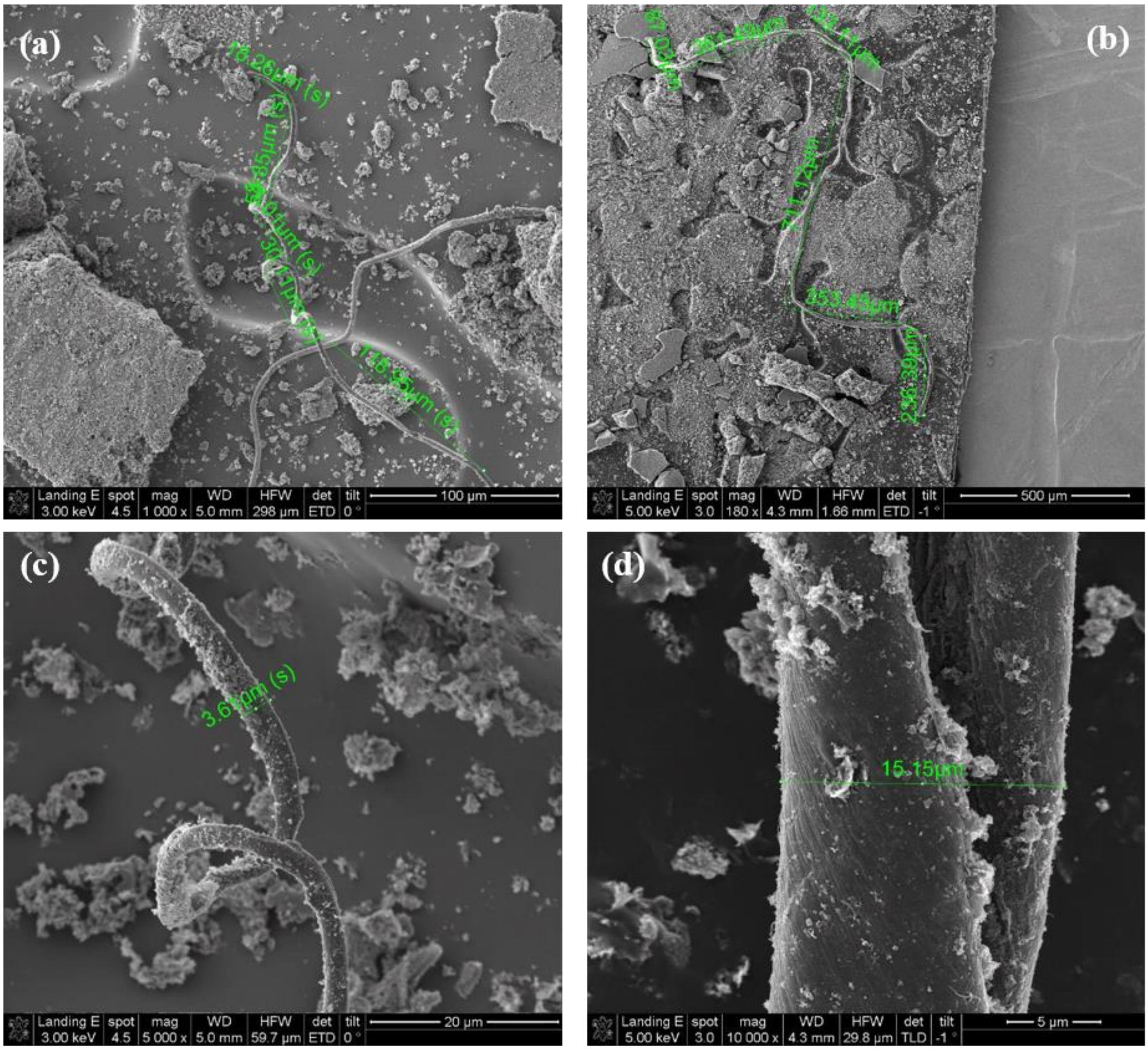

Figure S2. SEM images of CC10 to measure the fiber length and diameter.

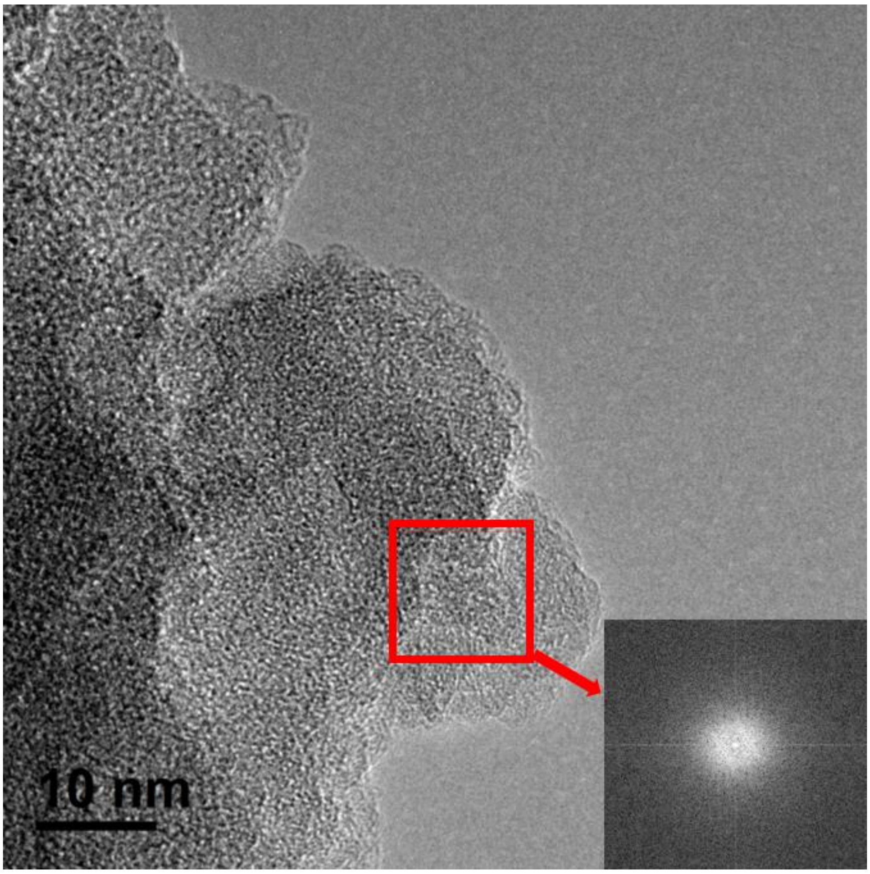

Figure S3. TEM image of BPC (The inset is the FFT pattern indicating the amorphous phase of BPC).

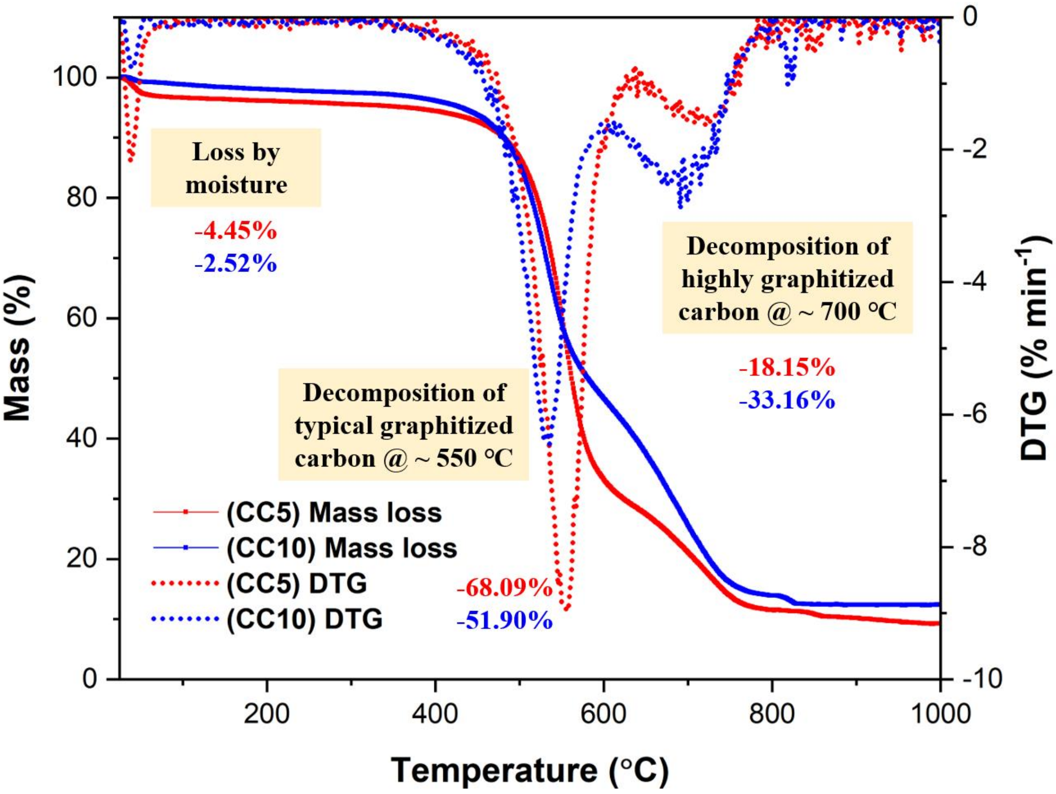

Figure S4. TGA and DTG plots of CC5 and CC10.

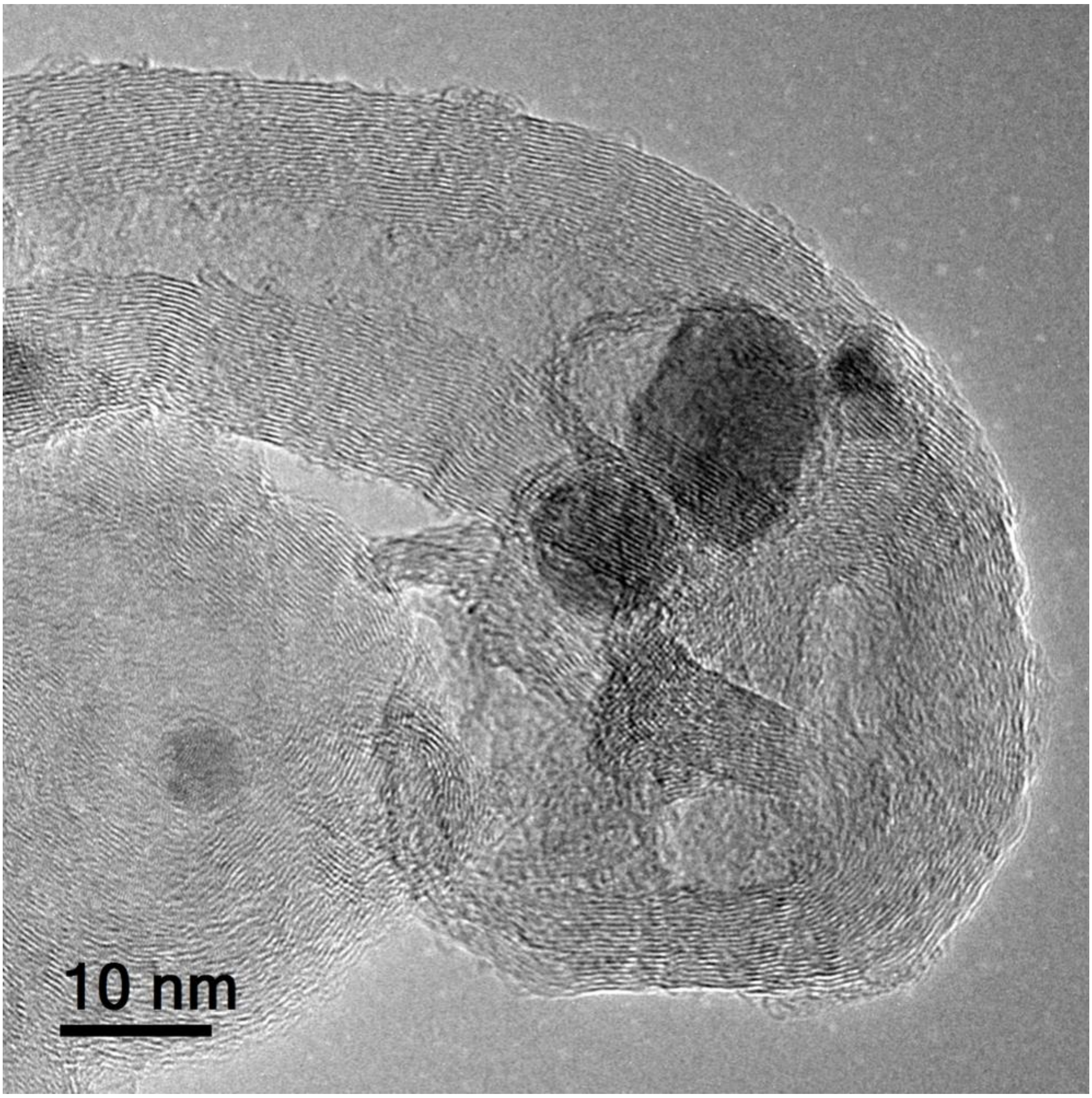

Figure S5. TEM image showing a Ni catalyst trapped inside a CNT. If the graphitic layer is thick, the Ni catalyst is not completely removed by hydrochloric acid during the washing process.

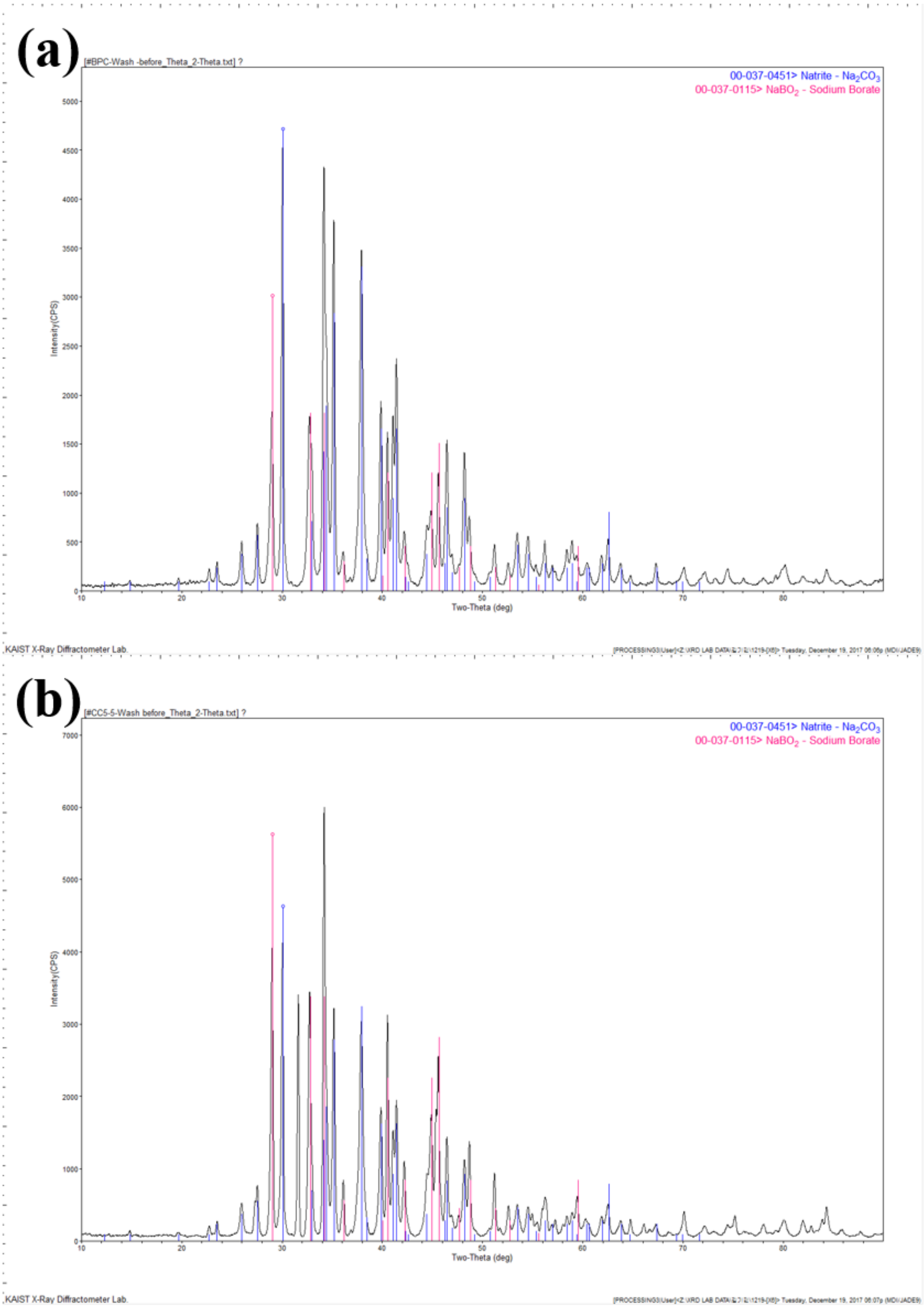

Figure S6. XRD plots of solid products after CO_2 conversion without a washing process: (a) $NaBH_4$ alone case and (b) mixture of $NaBH_4$ and $NiCl_2$ case. The plots show that the solid products in addition to carbon after the CO_2 conversion are $NaBO_2$ and Na_2CO_3.

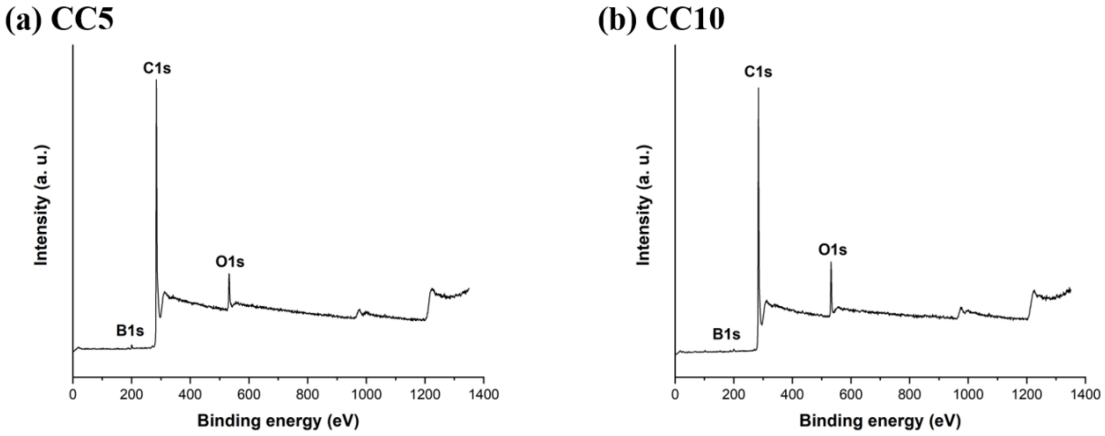

Figure S7. XPS survey plots of (a) CC5 and (b) CC10.

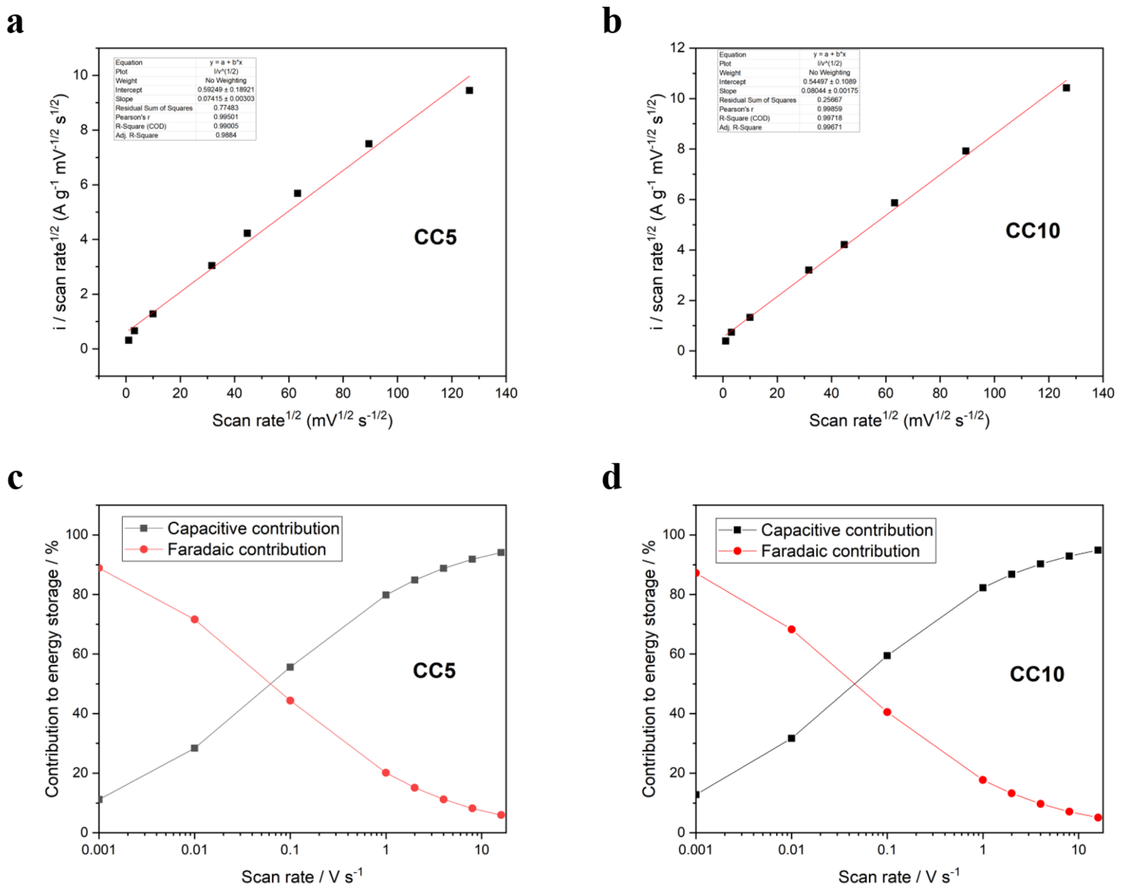

Equation	y = a + b*x
Plot	I/v^(1/2)
Weight	No Weighting
Intercept	0.59249 ± 0.18921
Slope	0.07415 ± 0.00303
Residual Sum of Squares	0.77483
Pearson's r	0.99501
R-Square (COD)	0.99005
Adj. R-Square	0.9884

Equation	y = a + b*x
Plot	I/v^(1/2)
Weight	No Weighting
Intercept	0.54497 ± 0.1089
Slope	0.08044 ± 0.00175
Residual Sum of Squares	0.25667
Pearson's r	0.99859
R-Square (COD)	0.99718
Adj. R-Square	0.99671

Figure S8. (a, b) The determination of the k_1 and k_2 at 1.0 V. (c, d) Contribution ratios of capacitances from the capacitive behavior and faradaic (redox) behavior at various scan rates.

Total charge storage in an electrode consists of capacitive (non-faradaic) and faradaic contributions. According to the power–law relationship, the ratio of capacitive contribution can be obtained by separating the current (i) (based on the CV analysis) into capacitive (k_1v, v: scan rate) and faradaic behavior ($k_2v^{1/2}$) as follows: $i = k_1v + k_2v^{1/2}$. Then, the k_1 and k_2 constants at various potentials can be determined by plotting $i/v^{1/2}$ versus $v^{1/2}$.

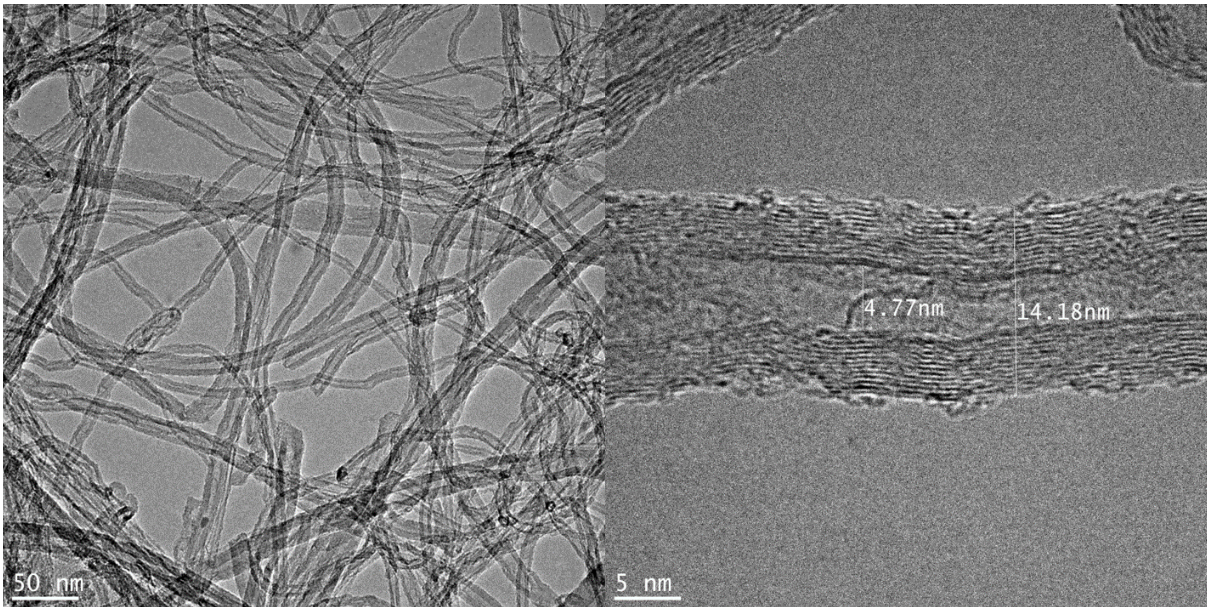

Figure S9. TEM images of commercial MWCNT.

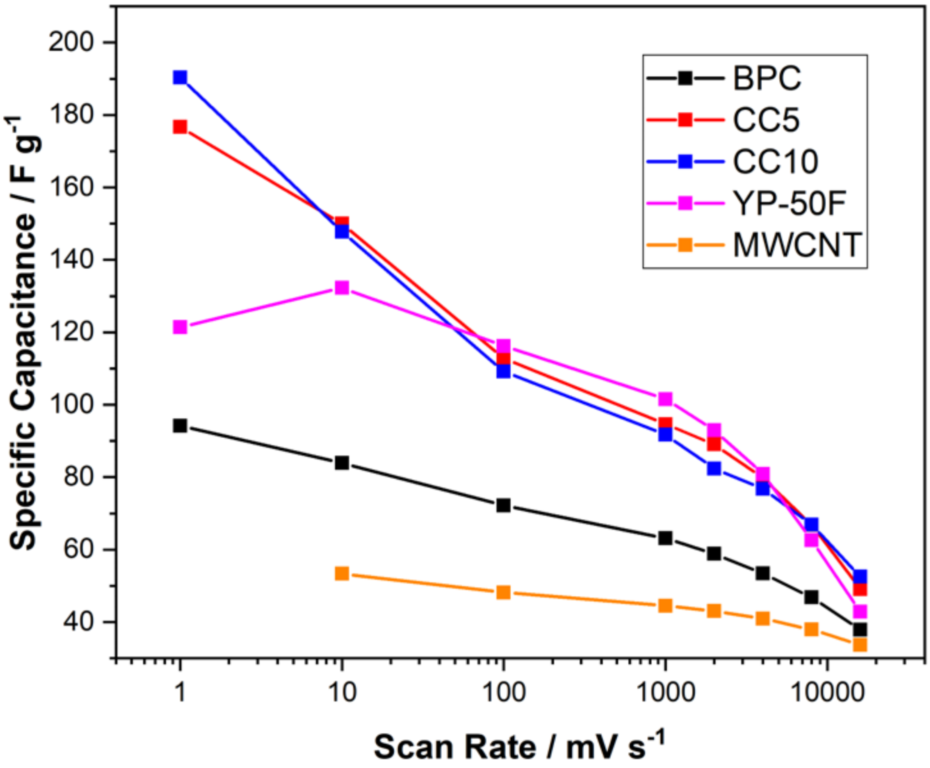

Figure S10. Specific capacitance calculated from the CV plots depending on scan rates.

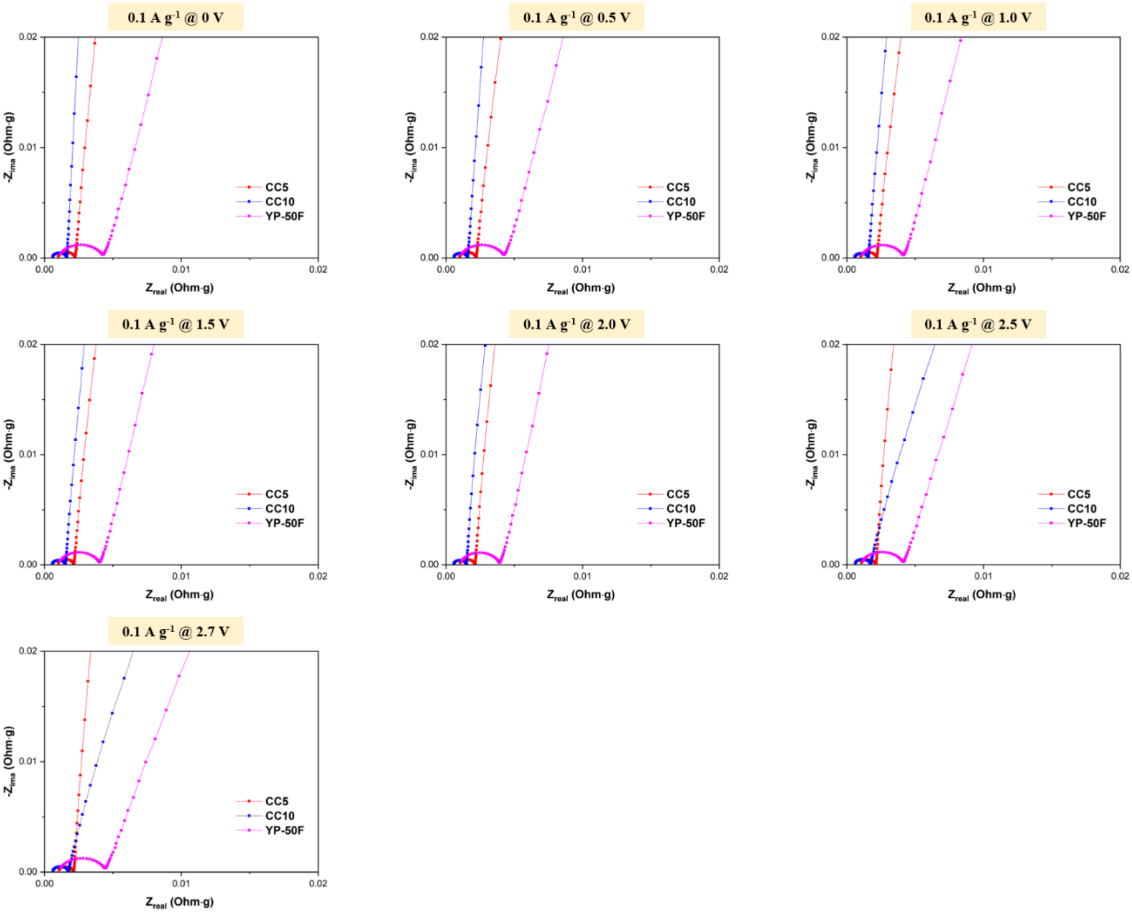

Figure S11. Normalized Nyquist plots obtained during charging up to 2.7 V at 0.1 A g^{-1}.

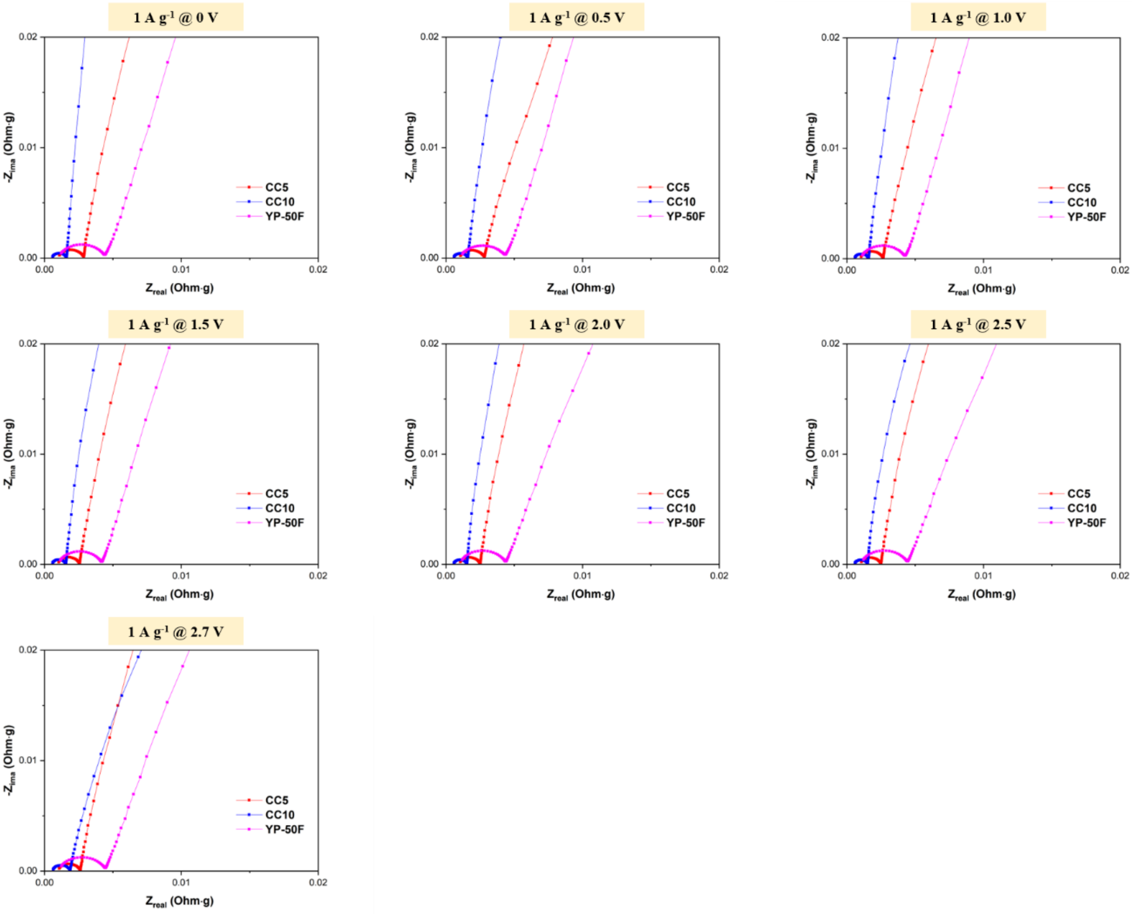

1 A g^{-1} @ 0 V

1 A g^{-1} @ 0.5 V

1 A g^{-1} @ 1.0 V

1 A g^{-1} @ 1.5 V

1 A g^{-1} @ 2.0 V

1 A g^{-1} @ 2.5 V

1 A g^{-1} @ 2.7 V

Figure S12. Normalized Nyquist plots obtained during charging up to 2.7 V at 1 A g^{-1}.

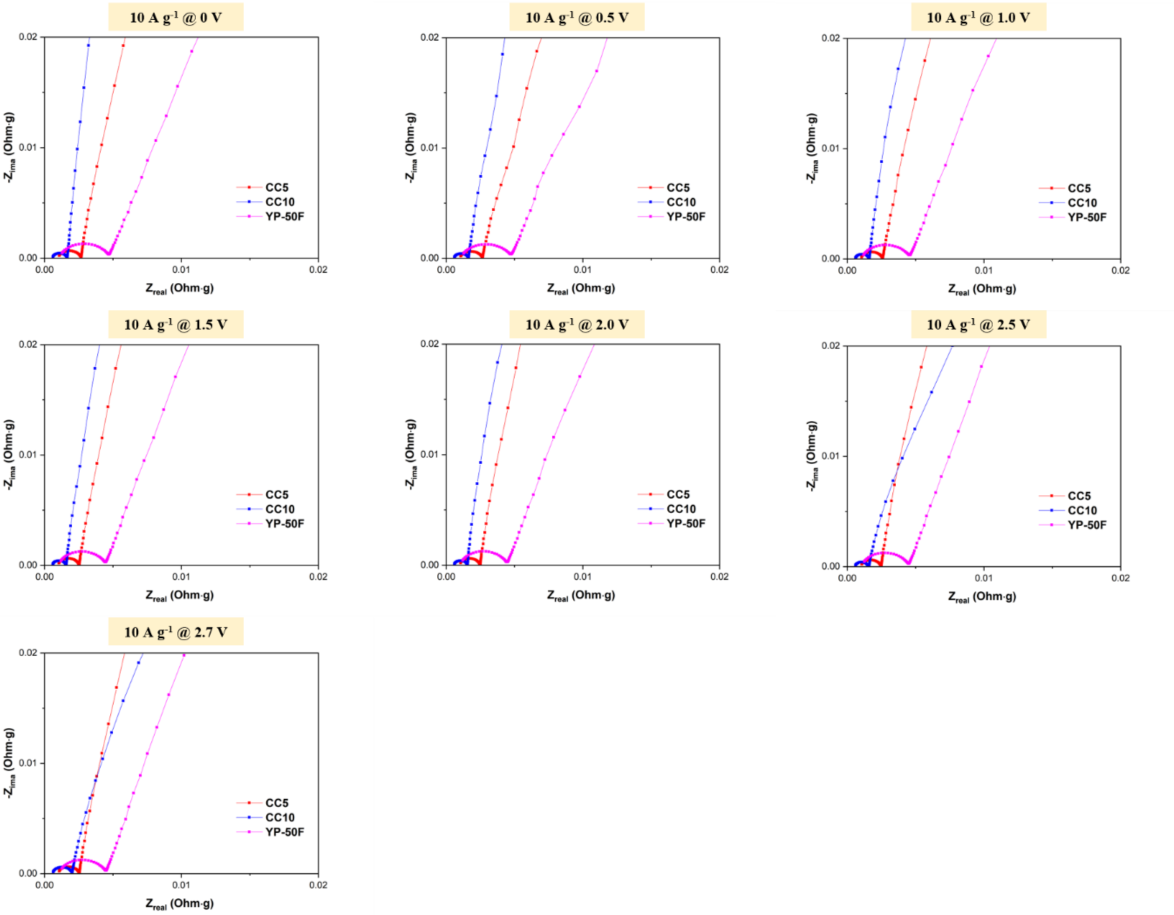

Figure S13. Normalized Nyquist plots obtained during charging up to 2.7 V at 10 A g^{-1}.

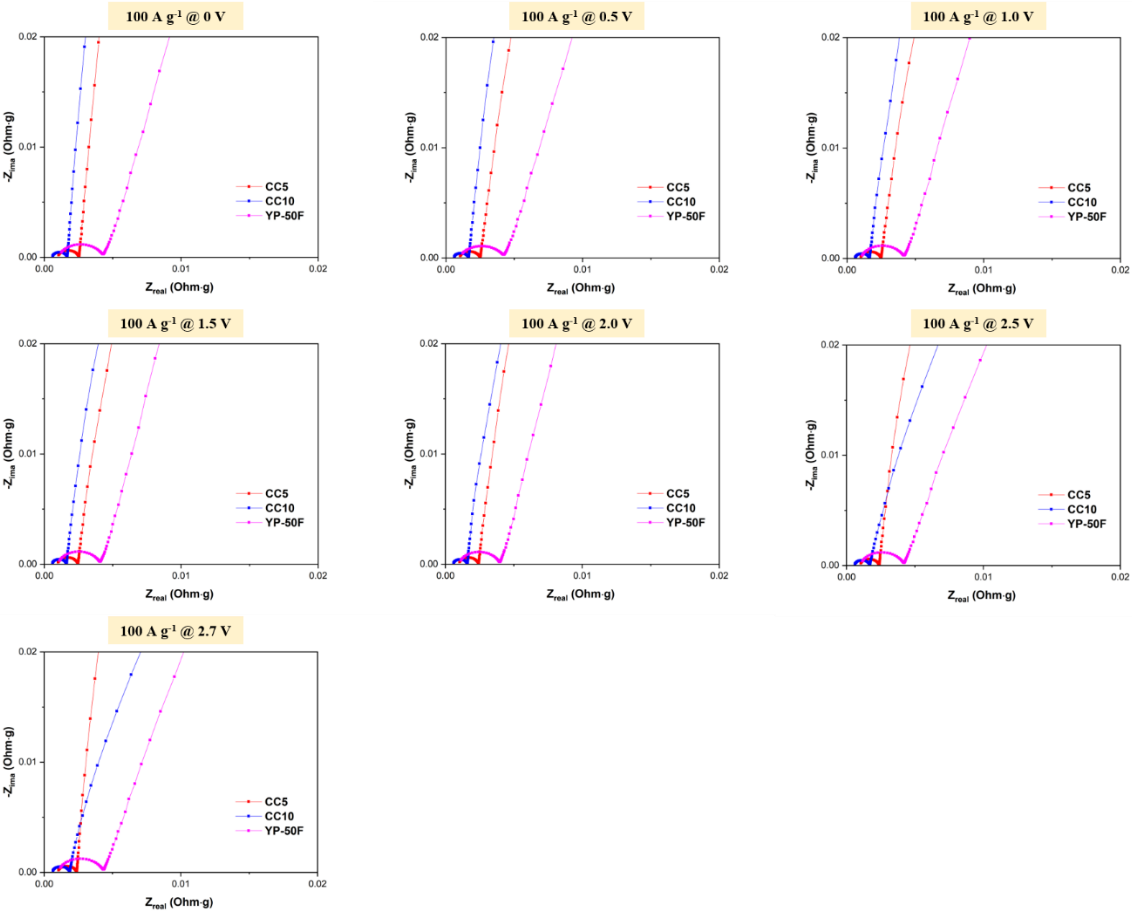

Figure S14. Normalized Nyquist plots obtained during charging up to 2.7 V at 100 A g^{-1}.

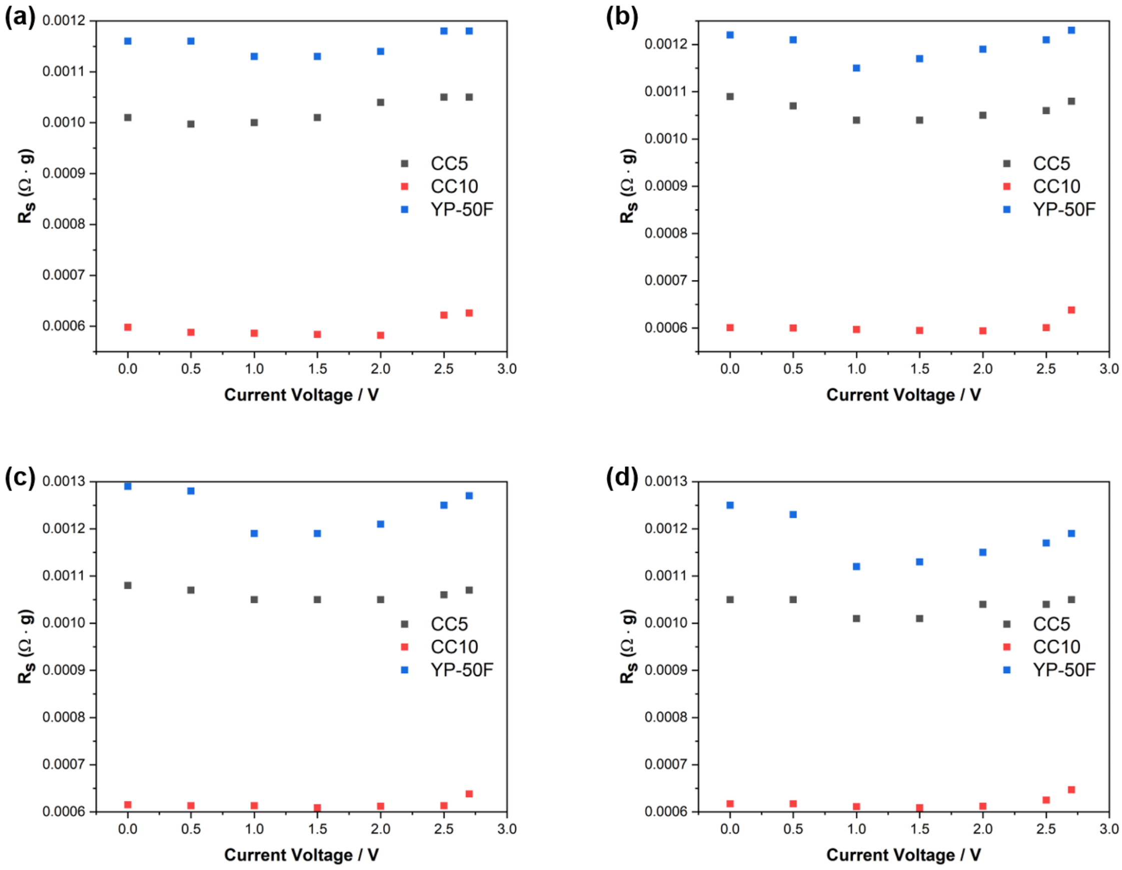

Figure S15. Measured series resistance (Rs) of all samples, derived from in situ EIS at several current densities of (a) 0.1, (b) 1, (c) 10, and (d) 100 A g^{-1}.

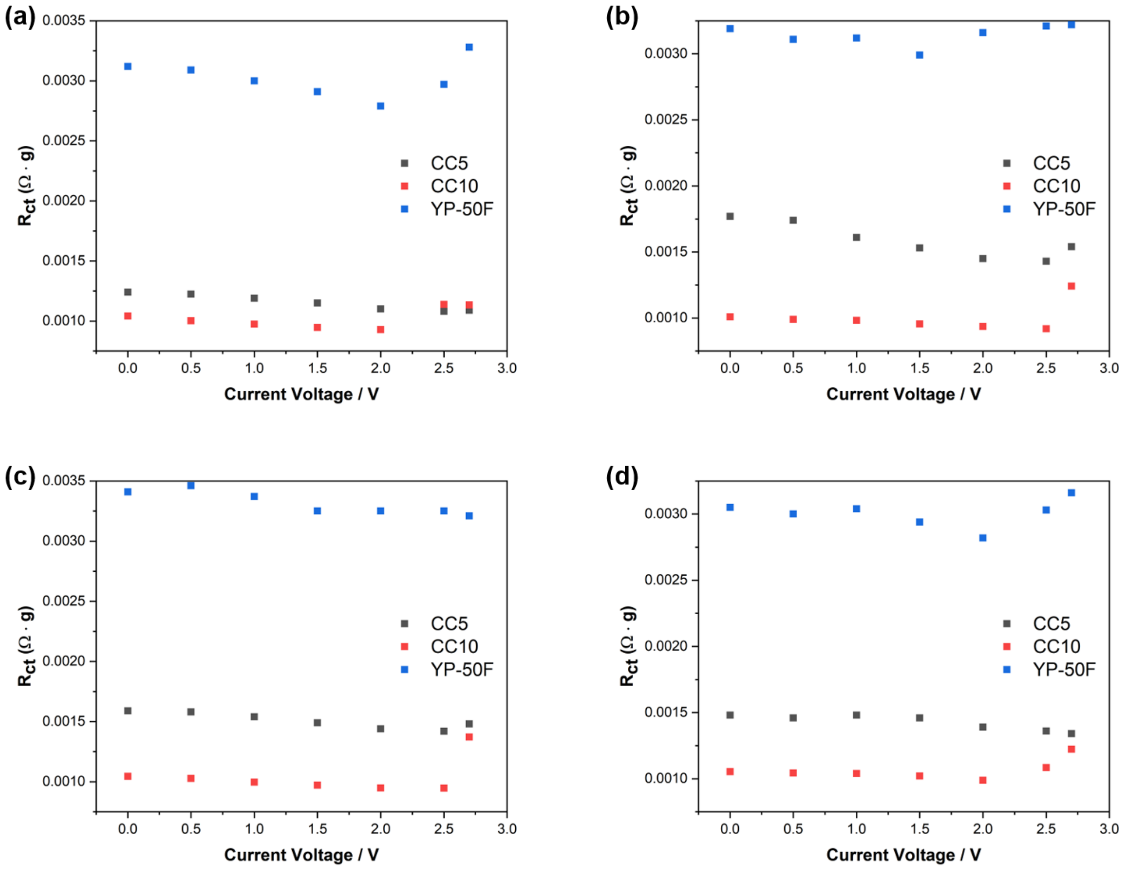

Figure S16. Measured charge transfer resistance (Rct) of all samples, derived from in situ EIS at several current densities of (a) 0.1, (b) 1, (c) 10, and (d) 100 A g^{-1}.

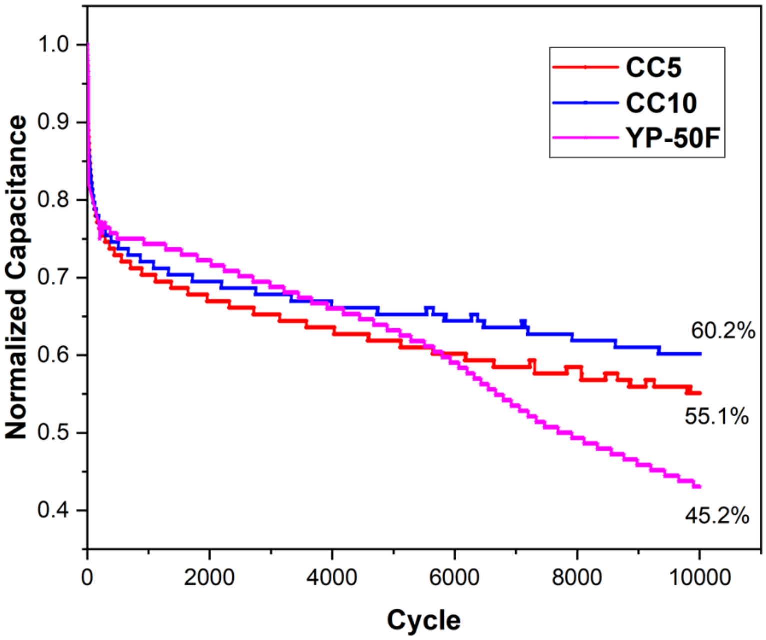

Figure S17. Stability test at 10 A g^{-1} under 65 ℃.

Table S1. The summary of Raman spectra of each sample.

Sample	D band (cm^{-1})	G band (cm^{-1})	2D band (cm^{-1})	I_D/I_G	I_{2D}/I_D
BPC	1360.2	1589.7	-	sp^2 amorphous dominant phase	
CC5	1347.9	1577.1	2686.1	1.01	0.24
CC10	1347.9	1578.4	2686.1	0.90	0.42

Table S2. The summary of surface element based on XPS survey.

Sample	C1s (at.%)	O1s (at.%)	B1s (at.%)
BPC	67.14 (1.96)[a]	15.24 (0.75)	17.62 (1.52)
CC5	91.65 (0.32)	7.32 (0.49)	1.03 (0.18)
CC10	88.76 (1.06)	10.24 (1.05)	1.00 (0.13)

a: Standard deviation, SD.